Journal of Archaeological Science 69 (2016) 64–74

Contents lists available at ScienceDirect

Journal of Archaeological Science

journal homepage: http://www.elsevier.com/locate/jas

Automated feature extraction for prospection and analysis of monumental earthworks from aerial LiDAR in the Kingdom of Tonga

Travis Freeland [a, *], Brandon Heung [b], David V. Burley [a], Geoffrey Clark [c], Anders Knudby [d]

[a] Department of Archaeology, Simon Fraser University, Education Building 9635, 8888 University Drive, Burnaby, BC, V5A 1S6, Canada
[b] Department of Geography, Simon Fraser University, 8888 University Drive, Burnaby, BC, V5A 1S6, Canada
[c] Department of Archaeology and Natural History, The Australian National University, 5205 H C Coombs Building, Canberra, ACT, 0200, Australia
[d] Department of Geography, Environment, and Geomatics, University of Ottawa, Simard Hall 047, 60 University, Ottawa, ON, K1N 6N5, Canada

ARTICLE INFO

Article history:
Received 10 December 2015
Received in revised form
18 March 2016
Accepted 7 April 2016
Available online 19 April 2016

Keywords:
Settlement patterns
Monumental architecture
LiDAR remote sensing
Automated featured extraction
Kingdom of Tonga
Grave mounds
Landscape archaeology

ABSTRACT

Recent LiDAR (Light Detection and Ranging) survey in Tonga has documented a dense and complex archaeological landscape, particularly on the principal island of Tongatapu. Among the features revealed by the LiDAR are a profusion of earthen mounds, most of which are associated with residence, sporting, or burial in the period 1000–1850 CE. For identification and mapping of the mounds we use and evaluate two automated feature extraction (AFE) techniques, object-based image analysis and an inverted pit-filling algorithm ("*iMound*"). Accuracy of these methods was measured using an F1-score (harmonic mean of precision and recall). Variable AFE results indicate that continual and iterative fine-tuning is required. Successful mapping of some 10,000 mounds on Tongatapu reveals a distinct spatial structure that relates to traditional land division and tenure.

1. Introduction

Aerial LiDAR technology is fundamentally changing the way archaeological survey is conducted around the world (Chase et al., 2012). Survey using LiDAR provides more extensive ground coverage than is possible with pedestrian survey methods; it also gives archaeologists the ability to peer beneath dense forest canopy, sometimes revealing spectacular anthropogenic landscapes. Detection of architecture and microtopographic alterations over wide swaths of land can have a profound effect on our understanding of the "spatial element" of human societies. It allows us to shift focus from a local scale to a regional scale, providing archaeologists with unprecedented geospatial contextualization for individual features in a cultural landscape.

The island of Tongatapu in the Kingdom of Tonga (Fig. 1) had a densely populated landscape and a politically complex dynastic chiefdom beginning no less than 1000 CE (Burley, 1998; Clark and Reepmeyer, 2014). Political complexity is marked on the land by large chiefly tombs as well as a widespread distribution of chiefly sitting mounds, earthwork fortifications and various-sized burial mounds in which non-élites are interred. While some mounds are monumental in scale (>10 m high), many of these mounds are low-lying features (<50 cm) and are often concealed by vegetative ground cover. Traditional methods of pedestrian and aerial survey are thus time-consuming to implement and leave substantial questions on survey accuracy. Employing recently acquired LiDAR for Tongatapu, we apply, evaluate and compare two automated feature extraction (AFE) techniques for mound identification, characterization and mapping. The spatial patterning of monuments on Tongatapu extracted from the LiDAR data can then be examined as a politically structured landscape reflecting internal complexities and organization of the dynastic Tongan chiefdom.

2. Background

2.1. LiDAR in archaeological practice

In aerial LiDAR, laser pulses are fired downward from an aircraft and reflect from the ground surface as well as objects on the ground

* Corresponding author. Present address: 6408 34 Ave NW, Calgary, AB, T3B 1N1, Canada.
E-mail address: tfreelan@sfu.ca (T. Freeland).

http://dx.doi.org/10.1016/j.jas.2016.04.011
0305-4403/

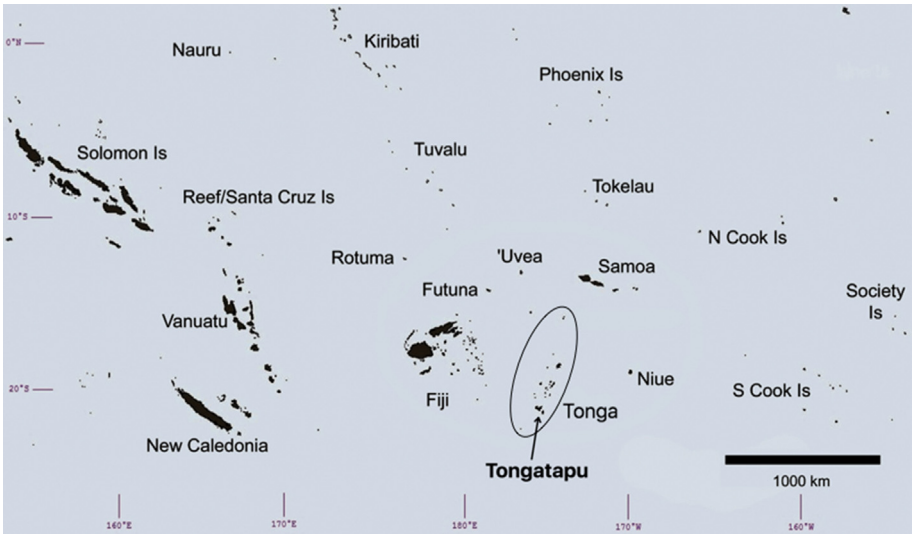

Fig. 1. Map of Tonga in West Polynesian context.

(trees, buildings). Reflected pulses are detected and the location of the reflected surface is established (Glennie et al., 2013). These datasets are processed to generate digital elevation models (DEM), which can be visualized to reveal different topographic features (Fernandez-Diaz et al., 2014). In archaeology, LiDAR is now frequently used for visualization of known sites, and for prospection of landscapes for previously unrecorded sites. A series of recent high profile discoveries have brought this technique to the attention of archaeologists and a captivated public. Examples include the discovery of the totality of the Caracol urban landscape by Chase et al. (2012); the detection of previously unrecorded urban centres in Cambodia (Evans et al., 2014); and the continued use of aerial LiDAR to reveal the full context of Stonehenge within a local monumental landscape (e.g., Bewley et al., 2005).

Survey using LiDAR can be particularly helpful in areas that are otherwise inaccessible for logistical, environmental, or political reasons. Rochelo et al. (2015) used LiDAR to document earthworks in Florida's challenging everglades environment. Recent studies employing LiDAR have also brought the "geospatial revolution" to South Pacific archaeology. Ladefoged et al. (2011) employed LiDAR in their analysis of the leeward Kohala field system in Hawai'i. Field alignments and trails were manually digitized in order to document the development of agricultural infrastructure in relation to agricultural potential productivity. McCoy et al. (2011) additionally mapped field systems in the northern Kohala district using LiDAR. Recently, Quintus et al. (2015) used LiDAR and semi-automated feature extraction to document artificial terraces in the hilly terrain of Ofu and Olosega in Samoa, combining their GIS analysis with systematic "ground truthing".

2.2. Automated feature extraction

For general usage of LiDAR in archaeological prospection, individuals with expert regional knowledge visually inspect DEMs to locate features of archaeological interest. Increasingly, however, automated GIS-based analyses are being developed to make digital prospection as effective as possible. These include the suite of techniques referred to as automated feature extraction (AFE), which are well developed in the field of computer-based image processing, but are relatively new for archaeological purposes (e.g., Luo et al., 2014). In large spatial datasets, AFE can be advantageous in that it applies objective criteria (e.g., roundness, relative elevation, etc.) for features of interest over vast survey areas.

Automated feature extraction algorithms can be developed for any type of remote sensing data. In the case of LiDAR, the 3-dimensional "point cloud" data acquired using LiDAR devices are processed and used to create high-resolution bare-earth DEMs. The AFE algorithms themselves consist of a series of classification rules, employing subjective contextual and geometric criteria to distinguish features of interest from other features on the landscape (the DEM "image"). In cases where features of interest in a survey area are relatively uniform in their shape and dimensions, and where the geology of the underlying landscape is neutral relative to the targeted features, AFE programs can be used to "extract" all cases of landforms that fit the set criteria. This study employs two AFE techniques that differ in their approach but share this fundamental definition.

Detection of anthropogenic relief in LiDAR-derived datasets has been achieved using a variety of techniques, most of which involve a form of template matching (e.g., Luo et al., 2014; Schneider et al., 2014; Trier and Pilø, 2012). The success of these and other related approaches centres on the fact that regular geometric shapes (squares, circles, straight lines) rarely occur in nature (Kvamme, 2013:55). For example, Trier et al. (2009) and Trier and Pilø (2012) detected circular features in Norwegian satellite imagery and LiDAR data by constructing circular templates of various sizes. Riley (2009) similarly developed a conical mound detection model, achieving nearly 90% success rate in detecting prehistoric burial features in the US Midwest.

The trend toward automation is a result of larger and more complex datasets becoming available, but their application to archaeological problems has been met equally with enthusiasm and skepticism as their results are of variable quality (Cowley, 2012). With continual and iterative development, however, AFE can be a powerful tool where automated techniques have been employed with increasing success in archaeological research (e.g., De Laet et al., 2007; Luo et al., 2014; Riley, 2009; Schneider et al., 2014; Trier et al., 2009; Trier and Pilø, 2012).

Like other "coarse" research methods, the value of AFE lies in its ability to reveal broad and otherwise undetectable patterns. Automated detection benefits prospection in large datasets where manual/visual inspection is considered to be too subjective, cumbersome, or time-consuming. In studying the Tongan archaeological landscape, we considered AFE a worthwhile endeavour

because earthen mounds are ubiquitous across the Tongan landscape. The natural landscape is very flat, so it is unlikely that natural hills will be mistaken for archaeological mounds. We observed that mounds on the principal island on Tongatapu tend to occur in spatially discrete clusters, or "mound fields", which likely relate to the traditional system of land division and tenure. Thus, the extraction of these features in their totality was considered an important first step in modelling the relationship between monumental architecture and socio-political developments in late prehistoric Tonga.

2.3. Study area and archaeological context

The Kingdom of Tonga is a West Polynesian archipelago comprising 167 islands in a northeast–southwest orientation (Fig. 1). The islands are a combination of low coral islands, sand cays and steep-sided volcanic high islands. The southern island of Tongatapu, a raised coral limestone island, was the centre of chiefly political power in the past. Tongatapu is the largest island in Tonga, being 34 km in length with a spatial extent of just over 259 km^2. Its surficial geography is flat to gently rolling, with soils derived from rich volcanic tephra, capable of supporting intensive and extensive agricultural production. This relatively featureless landscape makes Tongatapu an ideal candidate for AFE; the algorithms used in this study would be less effective at identifying archaeological features in more rugged terrain. The island is planted nearly from end to end, where natural forests have been replaced by a traditional system of mixed tree and root crop plantations. This agricultural regime, combined with near-ubiquitous prehistoric monumental and community-scale earthworks, makes Tongatapu a near-complete anthropogenic landscape. With regard to LiDAR data recording, the relative lack of dense forest canopy on Tongatapu has resulted in the creations of particularly accurate DEMs.

Prior to European contact, Tongan society was a highly stratified, geographically integrated chiefdom and one of the most politically complex societies in the Pacific. At its peak, the Classical Tongan Chiefdom (ca. 1000–1850 CE) consolidated authority in the archipelago and expanded its regional influence over West Polynesia and beyond. Powerful hereditary chiefs controlled land use and production under the centralized hegemony of the Tu'i Tonga dynasty. The archaeological record associated with this period is characterized by a proliferation of monumental and smaller-scale constructions including tombs, mounds, fortifications, and other earthworks (Burley, 1998). The modern Tongan landscape, relatively free of large-scale development, has preserved this architectural legacy. Earthen mounds are, by far, the most abundant feature class on Tongatapu, and the focus of our present analysis (Fig. 2).

Functional classification of mounds is difficult, even with excavation. Though many of these structures served as burial places for the Tongan chiefs and their retainers, some are associated with élite activities and visible displays of chiefly prerogative in life (Kirch, 1988:46; McKern, 1929; Swanson, 1968). The largest and best-studied monuments are the stone-faced sepulchres (*langi*) of the Tu'i Tonga at the ancient capitals of Heketa and Mu'a (Clark et al., 2008; Clark, 2014). Other élite constructions include chiefly sitting or resting mounds (*'esi*) and pigeon-snaring mounds (*sia heu lupe*) as well as the excavation of large conical water wells for chiefly bathing. However, the relationship between societal status and the vast majority of unadorned round or rectilinear earthen mounds, known variably as *fa'itoka* or *mala'e*, is less clear. The dimensions of these mounds vary, but most are at least 20–30 m in diameter and 40–50 cm in height, with some reaching heights of 10 m or more. On the basis of their sheer numbers, most "generic" mounds in Tonga are assumed to be burial places for subordinate chiefly and commoner lineages. Excavation of two of these mounds at 'Atele in Tongatapu by Davidson (1969) recovered 129 individuals, indicating continued use of these sites over time.

Fig. 2. A typical Tongan earthen mound without elaborations (e.g., stone facing). This mound is approximately 3 m high.

Many of the archaeological features revealed through LiDAR survey on Tongatapu appear to be concentrated in discrete zones, bounded by areas that are relatively free of earthwork construction. Although political boundaries associated with the chiefdom period have changed over time, many of the hereditary land holdings of the modern Tongan nobles are coincident with this distinct patterning. Part of the rationale for employing AFE to map earthen mounds was to generate a near-complete picture of this distribution, and to use that as a basis for investigating the geopolitics of the more distant Tongan past.

3. Materials and methods

Dense vegetation, property lines, and others factors that limit pedestrian survey have in the past hindered a full picture of the distribution of Tongan mounds. The present LiDAR dataset, therefore, represents a first opportunity to view the form and distribution of prehistoric monuments in their totality.

The objective of this study was to reveal the distribution of mounds on Tongatapu. The mapping of mounds required us first to recognize mound morphologies in the LiDAR dataset and translate those attributes into AFE protocols. The LiDAR dataset, and coincident orthophotos, were acquired during six flights in October 2011, and covers all of Tongatapu, Lifuka, and Foa with a point density greater than four points/m^2 overall (ground + non-ground points). The ALTM Orion M200 used in the LiDAR survey can capture a minimum of four returns for each pulse, with a vertical accuracy of ±15 cm. For this study, the raw LiDAR data had been pre-processed into a 1 m^2 resolution bare earth raster DEM, with vegetation and anthropogenic structures removed in order to portray only the ground surface (AAM, 2011). The value in each raster cell quantifies that cell's elevation above mean sea level. The LiDAR data was funded by AusAid as part of the Australian Government's project "Capacity building for Tsunami risk assessment in the South West Pacific". Permission to use the dataset for archaeological site recording was given by the Australian Government and the Government of Tonga to Burley and Clark.

3.1. Visualization, pre-processing, and calibration for AFE

Reference datasets were needed in order to provide a

comparison of the results from the two AFE procedures to reality for both calibration and validation purposes. In order to create those datasets, subjective manual delineation of mounds was performed using terrain derivatives generated from a DEM. To aid visual interpretation and detection of features in the DEMs, we experimented with various terrain derivatives such as hillshade, slope, and local relief modelling to highlight subtle anthropogenic traces (Fig. 3 — cf. Bennett et al., 2012; Challis et al., 2011; Hesse, 2010; McCoy et al., 2011; Štular et al., 2012).

Hillshade models, commonly used in archaeological prospection, provide a depth-perspective visualization to the 2-dimensional DEM by generating an artificial light source that accentuates topographic features. The slope visualization identifies terrain gradient surrounding each cell; areas with steeper sloping surfaces are coloured differently in the resulting raster. Since slope does not rely on an arbitrary light source, all features are highlighted regardless of their position on the landscape. Ideal DEM visualization was feature-specific; for example, hillshade and slope were used in conjunction to verify whether circular objects represented mounds or pits (Fig. 4).

Finally, high-resolution orthophotos were used to assess the positioning of features in relation to modern land use (Fig. 5). Fernández-Lozanoa et al. (2015) have recently utilized integrated LiDAR and orthophoto images to document the extent of Roman mining works in Spain.

In order to compare the strengths and weaknesses of the two AFE techniques, two identical sets of calibration data were generated through manual inspection of DEMs by delineating polygons around each mound located inside two arbitrary calibration zones on the island of Tongatapu. A third arbitrary validation zone containing 236 manually identified mounds, by which the results of AFE could be tested for accuracy, was also created (Fig. 6). We acknowledge that visual interpretation of the DEMs is subject to some level of error; in fact, we found that AFE identified a small number of features missed during manual classification.

3.2. Object-based image analysis (OBIA)

Detection of archaeological surface features from a bare earth raster DEM fundamentally requires a method for converting the set of elevation values in each cell into meaningful information about the presence or absence of a specific feature type. When the features are substantially larger than the size of an individual cell, as in our case, this method typically relies on the aggregation of multiple cells into objects that can be classified based on characteristics such as size, shape, texture and mean value, in an approach called object-based image analysis (OBIA).

LiDAR-derived DEMs may contain spatially un-correlated noise that obscures the true landscape signal and causes errors during the calculation of simple topographic derivatives such as slope and curvature, hence complicating any method of detecting the mounds (Li et al., 2011). Prior to the application of an AFE algorithm, data preprocessing was used to remove such noise. In our case, preprocessing for OBIA included application of a spatial filter from which the mean elevation, within a 100 m radius around each cell, was subtracted from that cell's original elevation value (see Hesse, 2010 for a discussion of filtering). The resulting data layer represents the individual cell's elevation relative to its surrounding area. Two additional data layers were created from the result, specifically to identify cells that form part of a mound of the size typical of the Tongan landscape. The mean relative elevation value within a 19 m radius was subtracted from the mean relative elevation value in an 11 m radius around each cell (henceforth: 11:19). This allowed cells on or near the top of small mounds to achieve high values because the 11 m radius would largely fall on the mound itself, while the 19 m radius would include the surrounding lower areas. A second data layer was created similarly using 23 m and 15 m circles instead (henceforth: 15:23), performing the same function for larger mounds.

The first step in a typical OBIA approach is image segmentation, which applies an algorithm that separates the image into internally homogeneous segments. The image segmentation algorithm used for this study was implemented using the *eCognition* software where three parameters (scale, shape, and compactness) were used to tune the algorithm based on a weighted combination of data layers (Baatz and Shäpe 2010). The three parameters and the number and kind of data layers used to quantify segment homogeneity are typically defined following a trial-and-error process, during which the user attempts to achieve a result where the image segments match landscape features as closely as possible. If successful, this allows segment characteristics to be used to determine which segments contain the feature of interest. Due to the range of mound sizes on Tongatapu, we were unable to define a combination of parameters, specifically a scale parameter, which would result in segments matching the majority of mounds. To overcome this problem, a very small scale parameter (0.5) was used, which allowed separation of the data into very small segments, none covering a whole mound. Segmentation was based on an equal combination of the 11:19 and 15:23 layers, with the shape parameter set to 0.1 and the compactness parameter set to 0.5.

The second step in OBIA is to pass the segments through a series of decision rules, which serve to merge or split segments, and assign class labels to segments, according to user-specified rules. As for the segmentation parameters, the development of a satisfactory

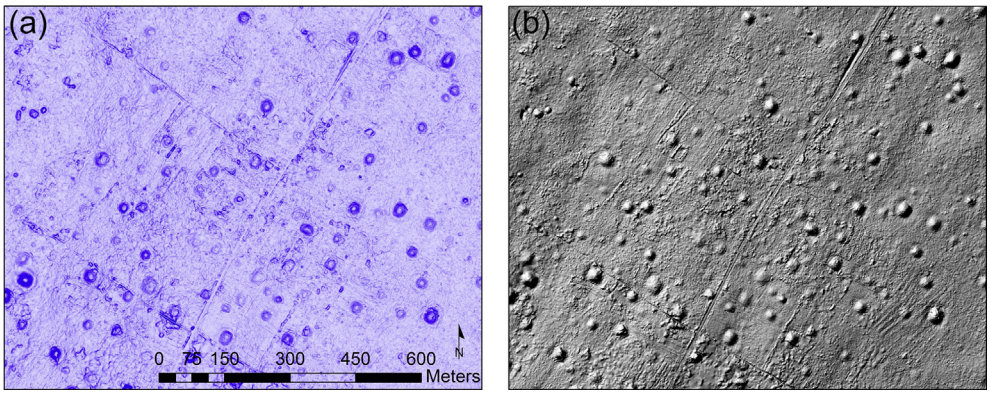

Fig. 3. Comparison of DEM visualizations for mound survey: (a) slope and (b) hillshade.

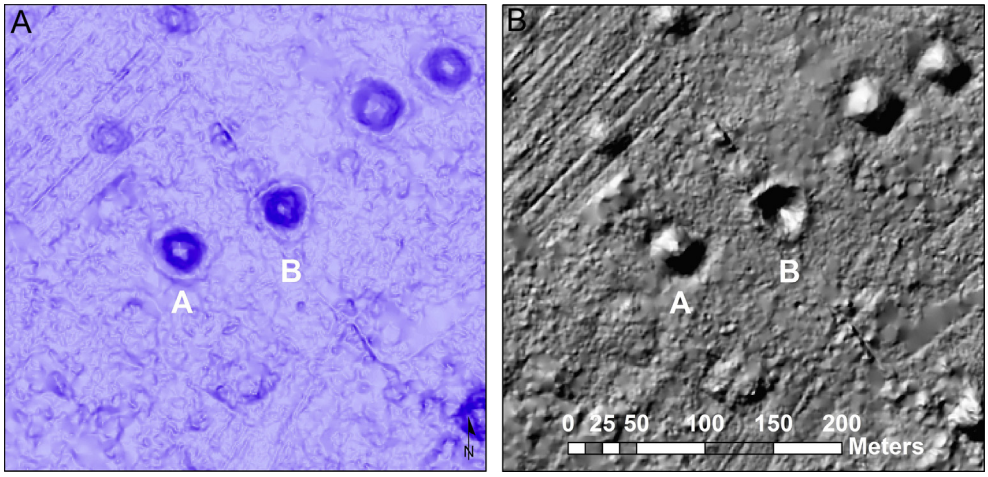

Fig. 4. Comparison of mound (A) and depression (B; freshwater well), using slope gradient (left) and hillshade (right).

Fig. 5. Hillshade model superimposed on aerial orthophoto. Note mound proportions relative to modern buildings.

rule-set is a user-intensive trial-and-error process, in which the results of one rule are inspected, and the rule modified or another added, until a satisfactory result is achieved. The resulting rule-set is specifically tailored to the unique characteristics of the landscape at hand. The rules developed for our study, which took approximately 10 h to develop, relied on the following types of segment characteristics:

- Elevation (segments with mean elevation ≤ 0 were considered to cover water, and were eliminated from the rest of the analysis)
- 11:19 and 15:23 (segments with high values in these layers were generally classified as mounds)
- The difference between the value of a segment and the mean value of all neighbouring segments, for layers 11:19 and 15:23

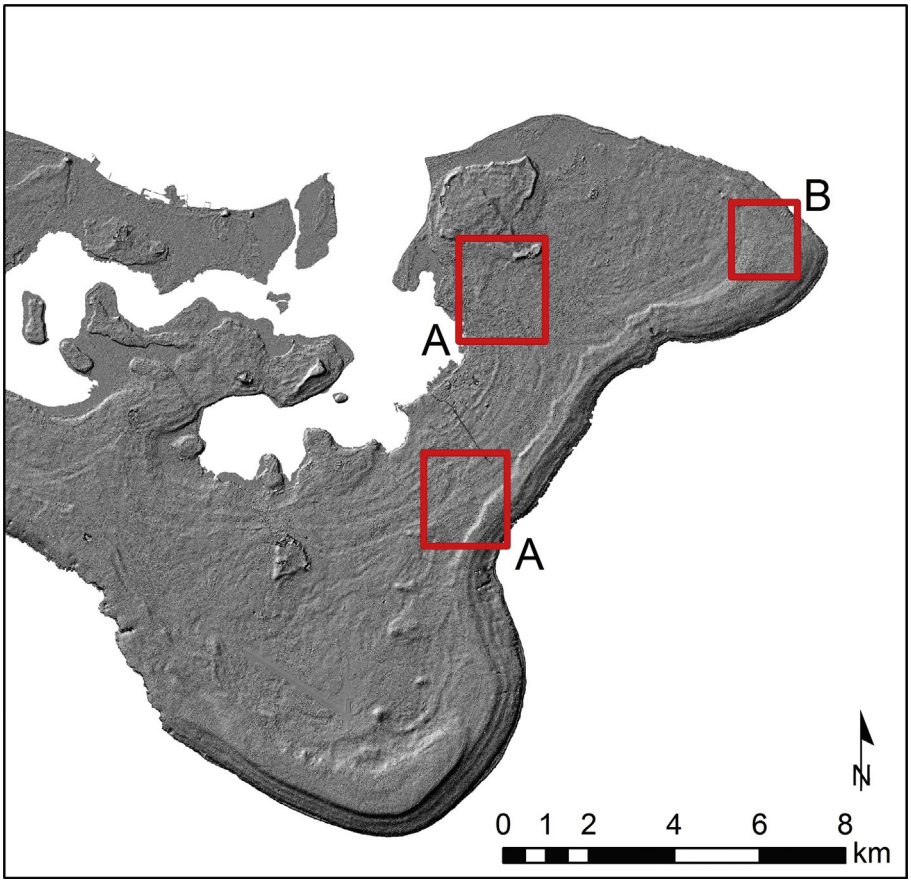

Fig. 6. Locations of calibration (A) and validation (B) zones.

(segments with values higher than their neighbours were generally classified as mounds if also satisfying other criteria. A similar criterion would not suit a hillier landscape)
- Area (segments smaller or larger than any known mounds were not classified as mounds, regardless of other characteristics)
- Roundness and Compactness (segments with complex shapes were generally not classified as mounds)

3.3. Inverted mound algorithm

The inverted pit-detection method (hereafter referred to as the *iMound* method — note that this algorithm is not affiliated in any way with Apple Inc.), an automated algorithm designed for this project and implemented in the *R* programming language (R Development Core Team, 2012), applies techniques from hydrologic modelling and geomorphometry to the detection of mounds. The basic procedure follows these steps: (1) the preprocessing of the LiDAR data; (2) the application of a pit-filling algorithm and detection of potential mounds (cf. Hanus and Evans, 2015); and (3) the application of morphometric rules to remove noise and non-mound features.

The first step of the *iMound* method was to apply a mean filtering procedure to the DEM that assigns the centroid pixel the value of the average values within a window size of f pixel, which causes the flattening of the noise from a DEM.

Mounds can be thought of as inverted pits or depressions within a landscape and as such, algorithms that have been used to identify closed depressions may be applied to the DEM if it were inverted first (i.e., flipped inside-out). In the hydrological modelling literature, several pit-filling algorithms have been developed (e.g., Planchon and Darboux, 2001; Wang and Liu, 2006) — for this study, the Wang and Liu (2006) algorithm was applied due to its ability to handle large datasets. Following this, a simple subtraction of the filled DEM from the inverted DEM resulted in a data layer of mound heights (Hanus and Evans, 2015).

In some cases, mounds may be found along a slope where the long-range topographic trend must be separated from the local patterns of the mound. As such, an optional secondary filtering using a mean filter with a window size of d pixels was applied to the mound height layer.

A variety of features were observed based on a visual assessment of the de-trended mound elevation where the final step was to separate the mound features from the non-mound features (i.e., buildings, remaining noise, and naturally occurring mounds with an irregular shape) using a series of thresholds/rules. The first threshold is the minimum mound height, h, which distinguishes potential mounds from naturally occurring terrain. h must be determined from the de-trended mound elevation layer rather than field measurements of mound height because the value of h is less than the actual height of the mounds due to the filtering procedure that was applied. The application of h results in a binary mound layer where values $> h$ were assigned a value of 1 and values $< h$ were assigned a value of 0 in a polygon format.

The majority of mounds are circular/conical. Using the binary mound layer, two additional thresholds were applied: mound circularity threshold, c, and minimum area of mound threshold, a. Due to the relatively uniform and circular shapes of the mounds, a circularity index, c, was calculated for each polygon in the following:

$$c = (4\pi \text{ Area}) \Big/ \text{Perimeter}^2, \quad (1)$$

where values of c close to 1 represent a perfect circular feature while values close to 0 represented an irregularly shaped feature.

There are a number of mounds that are sub-rounded or square-topped; it was found, however, that in most cases, natural slumping/erosional processes resulted an overall shape that fell within a relatively conservative circularity threshold. This threshold could be modified in future to detect mounds that are more square/rectangular in shape. In addition to mound circularity, an additional parameter for specifying the minimum areal extent of each mound, a, was also necessary in order to further separate the actual mounds from the noise that were in the form of small speckled features. The final output of the *iMound* algorithm consists of polygon outlines of the detected mound locations.

In order to identify the optimal values of the parameters for f, d, h, c, and a, the algorithm was applied to a DEM of the calibration area with known mound locations and internal validation was calculated based on the F1-Score (van Rijsbergen, 1979). A range of parameter values was tested, and the optimal result produced with the following values: $f = 15$, $d = 15$, $m = 0.06$, $a = 60$, and $c = 0.82$.

3.4. Accuracy assessment

Using the validation area, which consists of 236 manually identified mounds, the harmonic mean of precision and recall (the F1-Score) was calculated due to its suitability in validating binary classification problems where only true positives (TP), false negatives (FN), and false positives (FP) could be determined. The F1-Score is calculated as:

$$\text{F1} - \text{Score} = 2\text{PR}/(\text{P} + \text{R}), \quad (2)$$

where P is the precision:

$$\text{P} = \text{TP}/(\text{TP} + \text{FP}) \quad (3)$$

and R is the recall (or sensitivity):

$$\text{R} = \text{TP}/(\text{TP} + \text{TN}). \quad (4)$$

An F1-score of 1 represent a perfect classification, while scores closer to 0 represent poor classifications.

4. Results

We executed both AFE procedures in the validation zone and calculated their detection success rates. Both techniques performed reasonably well, with *iMound* achieving the higher F1-score (Table 1). Compared to OBIA, the rate of false positives was slightly higher in *iMound*, but fewer low, subtle mounds went unidentified. A subjective visual assessment of the results also confirmed that the *iMound* polygon output better reflected the actual shape and proportion of the mounds (Fig. 7), as OBIA tended to identify an irregular shape within the actual mound boundaries.

Table 1
Feature extraction validation results. OBS: manually identified mounds; DET: mounds detected by each technique; FN: false negatives; FP: false positives; TP: true positives.

	F1-Score	FN	FP	TP	OBS	DET	Precision	Sensitivity
OBIA	0.77	68	34	168	236	202	0.83	0.71
iMound	0.84	36	42	200	236	242	0.83	0.85

Both techniques were used to produce a nearly complete map of mounds on the island of Tongatapu.

4.1. Mound density and distribution

The OBIA algorithm detected 9418 mounds, while *iMound* detected 10,220 mounds (Fig. 7). As a result, we are confident in estimating the total number of mounds on Tongatapu at around 10,000. Radiocarbon dating suggests that the majority of mounds in Tonga were built after 1200 CE with mound construction rapidly diminishing in the 19th Century (Clark, 2015; Spennemann, 1989; Stantis et al., 2015). This suggests that an average of 14 mounds were built annually on Tongatapu during a mound construction phase that lasted seven centuries. Given the relatively small surface area of the island (259 km^2), this is a strikingly dense built landscape (approximately 39 mounds/km^2).

In spite of the differences between the two AFE approaches, the spatial distribution of mounds was broadly similar. Mound distribution, however, is highly uneven; as illustrated qualitatively using an isopleth map, produced by applying a kernel density estimation to all mounds detected by *iMound* (Fig. 8B).

The isopleth map provides a generalized view of relative mound concentration, indicating areas that are very densely built, as well as those with moderate or very little mound construction activity. The patterning was further analyzed using optimized hot spot analysis (Fig. 8B). Hot spot analysis uses the Getis-Ord Gi statistic to identify clusters of points and assign them a z-score. The z-score represents the statistical significance of the clustering (at 90%, 95%, and 99% thresholds) with a random distribution as the null. This analysis better delineates the most significant clusters and allows for the identification of specific nodes in the dataset.

Both the kernel density and the hot spot analysis provide a broad picture of the monumental landscape, with clusters likely representing political and settlement nodes. Neither spatial analysis accounts for mound type, size, or morphology. The pattern is thus “unweighted”; future research into morphometric and functional categories will add important nuance, showing the distribution of specific feature types relative to this overall distribution.

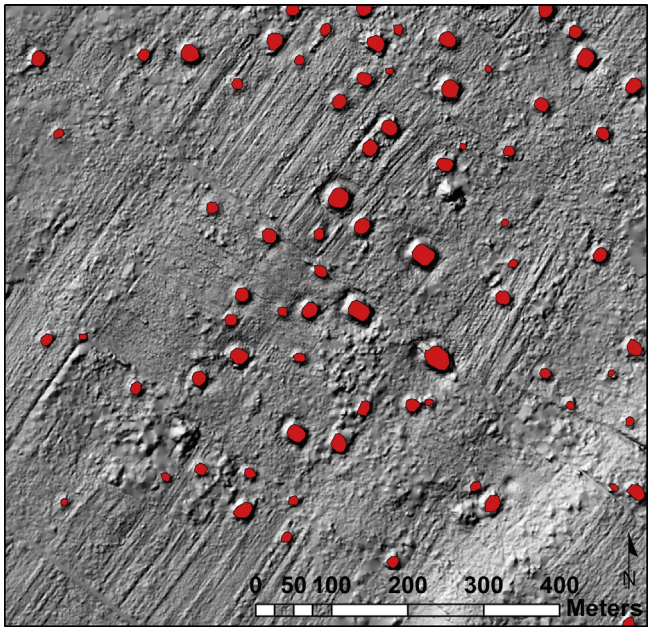

Fig. 7. Mounds detected using the *iMound* protocol. Diagonal striations in the model are the result of modern agricultural activities.

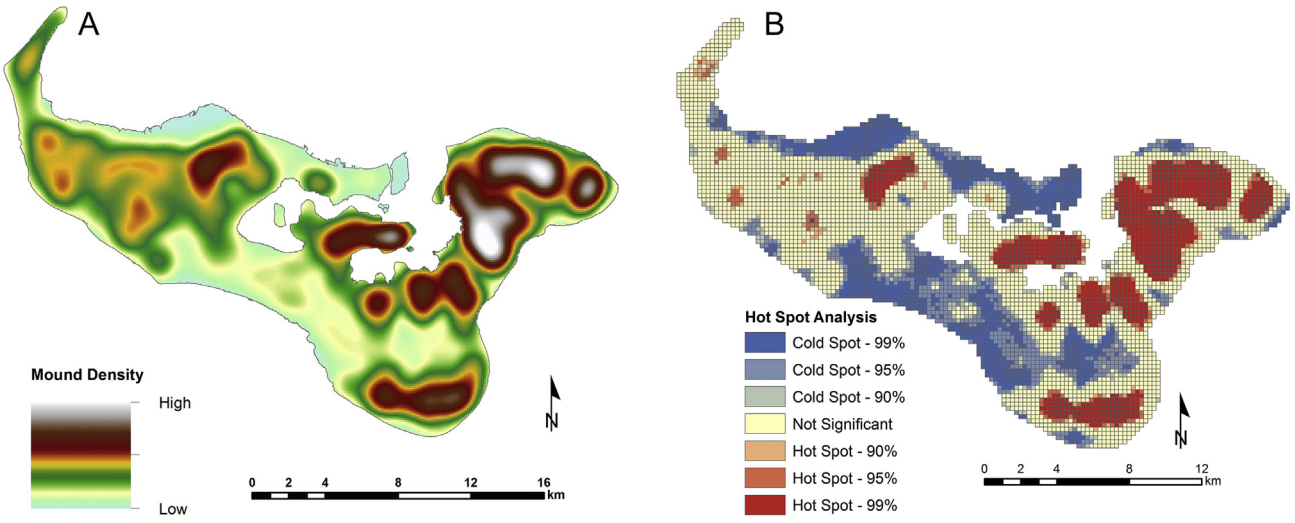

Fig. 8. A) Kernel density isopleth map of Tongatapu showing relative mound density; B) Getis-Ord hot spot analysis with statistical significance of clustering.

There are areas on Tongatapu that have been substantially altered for the construction of sporting fields, school grounds, and other facilities. Notably, the construction of Fua'amotu International Airport, which occupies a large area in the southern district of the island, very likely flattened a significant number of features. Spennemann (1989) surveyed this area and found a relatively dense concentration of mounds. Areas of low mound concentration were checked using orthophotos and visual examination indicates that modern or historical land disturbances were not responsible for patterns of relative mound absence visualized in Fig. 8.

5. Discussion and conclusion

In any AFE algorithm there is a fundamental trade-off between precision (the percentage of real mounds detected) and recall (the percentage of detection that are real mounds), and as a result neither technique was capable of detecting close to 100% of the real mounds (Table 1). However, it is important to note that the feature extraction techniques detected some features that were unidentified in visual inspection. As we developed and tested our AFE algorithms using mounds visually identified in the two calibration areas, it occurred on more than one occasion that an algorithm identified a feature that had not initially been identified as a mound, but was identified as such upon closer inspection. Assuming some mounds were also unidentified in the validation data, the number of false positives for each technique may be overestimated, and the true number of mounds on Tongatapu may be underestimated, in our study. The presence of false negatives is largely explained by the variability in mound form. Whereas a human observer can identify a mound with unusual morphological characteristics, an AFE algorithm searches for features that best fit its set of criteria and will exclude any mound that is unusually shaped, very flat, or occurs on excessively complex topography. We can conclude from this that neither visual interpretation nor automated detection are infallible; continual, iterative fine-tuning of these methods is essential.

While the identification of each individual mound is subject to some uncertainty, the utility of AFE in a landscape dense with relatively uniform features is in its ability to produce the general spatial distribution of mounds. Ground-truthing of the LiDAR in Tonga confirmed that apparent mounds on the DEMs are in fact real — in fact, the LiDAR is better in some cases than pedestrian survey for identifying subtle features in vegetated areas.

The pattern revealed in Fig. 8 is thus a unique starting point for understanding the Tongan political landscape — regardless of the absolute number of mounds. It allows visualization of the broad-scale spatial pattern of mound distribution, in which mounds tend to occur in dense, spatially discrete clusters, with areas of relatively unbuilt land in between. This is particularly the case in the central (Mu'a) and eastern (Hahake) districts of the island. Probably not coincidentally, our estimated density of 39 mounds/km^2 is close to the estimates arrived at by Spennemann (1989:283) for central and south-central Tongatapu through conventional pedestrian survey (36–38/km^2).

5.1. Methodological implications

This study has important implications for archaeological prospection employing high-resolution remote sensing data. With larger and more numerous high quality datasets becoming available, it is important that archaeologists work with remote sensing and geospatial data processing specialists to find better ways of analyzing them. Automated feature extraction is a response to the need for rapid and semi-quantitative landscape analysis, particularly in circumstances where large numbers of relatively uniform features are visible (e.g., Luo et al., 2014). Of course, the methods used here would require significant adaptation if used in more complex, rugged terrain.

Both OBIA and *iMound* were successful in extracting mounds on Tongatapu, with the former being the more conservative technique. Continuous fine-tuning could improve results in both cases. The relatively flat topography of Tongatapu likely contributed to the success of these techniques; however, mountainous or hilly terrain would pose greater problems for separating anthropogenic from natural relief. Both of these procedures could be modified to target mounds with variable morphologies; sub-rounded and square-topped mounds could be extracted in the future to determine their distribution. Additionally, estimates of volume, height, and basal and mound top area could be made in order to create size or shape classifications/hierarchies. This dataset allows us to pursue these goals in a way that has not been possible before with conventional recording methods.

On an island such as Tongatapu, manual correction of AFE outputs, paired with systematic “ground truthing”, could be conducted

on a case-by-case basis to create a master inventory of features. We see potential here for heritage management applications, particularly as high quality remote sensing datasets become publically available.

Prufer et al. (2015) have recently shown LiDAR to be insufficient for detecting small (1–3 m) anthropogenic structures under dense secondary growth, and have argued that LiDAR does not fully substitute traditional survey methods; our ground-truthing of the present LiDAR dataset in Tonga has shown, albeit anecdotally, that even very low mounds of less than 50 cm are accurately represented, even in densely vegetated areas of forest cropping (coconut, banana, yam, and kitchen-garden plants). The same mounds are almost imperceptible on the ground without substantial clearance of brush. Chase et al. (2011, 2014) recorded subtle structures of <25 cm in their LiDAR survey of dense jungle environments in Belize.

As several recent studies (e.g., Ainsworth et al., 2013; Quintus et al., 2015) have recently pointed out, pairing remotely sensed survey data with systematic ground truthing is critical. Study of remote sensing data prior to or during pedestrian survey can help to narrow the focus of fieldwork, and in turn, on-the-ground experience of an archaeological landscape is essential for understanding the context of individual sites and monuments. Certain key pieces of information — for example, the presence or absence of stone facing on an earthen mound — are completely overlooked in digital survey. Whereas conventional survey methods provide more detail, but at a smaller extent, digital methods provide "grainier" detail at a wider extent; it is in the thoughtful pairing of these strategies that archaeologists can find true value (Chase et al., 2011, 2014).

5.2. Implications for Tongan prehistory

It has been said that traditional politics in Tonga was "kinship writ large" (Urbanowicz, 1977); genealogical reckoning codified aspects of individual rank and seniority (Herda, 1988). Kinship also structured the settlement of lands. Prior to reforms in the 19th century, all land in Tonga belonged to high-ranking, titled chiefs, who apportioned smaller tracts to lesser chiefs. Individual land units (*'api*) were settled as compounds and occupied by extended families. *'Api* were well fenced, and a network of roads served to link but separate individual tracts. Related kin groups formed *kainga*, or clans, which provided labour for their ranking chief when required for building projects — projects such as earthen mounds. The term *fonu'a* was used to describe both a chief's hereditary land and the people who lived on it, the latter being arguably the more valuable resource (Bott, 1982:69).

The residential centres of the paramount Tu'i Tonga lineage have been treated in detail recently (Clark, 2014; Clark and Reepmeyer, 2014). This study represents a first step in documenting the archaeological legacy of the numerous subsidiary chiefly lines, as well as the settlement pattern of commoners.

Relatively little is known about the people who built and used the majority of generic, "lower-ranking" mounds, with only a handful having been excavated (Davidson, 1969; Spennemann, 1989). The construction of high-ranking mounds, however, employing *corvée* labour (Gifford, 1929:181), is widely interpreted as an affirmation of authority and rights to land, in addition to whatever other functions the monuments had (Burley, 1996, 1998:370; Clark and Reepmeyer, 2014; Kirch, 1990). Aside from their function as burial sites, many of the mounds highlighted in this study likely served as ritual sites for god worship, ancestor veneration, and reaffirmation of social ranking. Thus their distribution on the landscape is highly significant.

Our results show that mound patterning is non-random, with a tendency toward clustering interspersed with relatively "empty" areas (Fig. 8). Visual assessment shows that in some cases, these mound fields are separated by linear ditch-embankment features, described elsewhere as "sunken roads" (e.g., Burley, 1998:371; Spennemann, 1989) but probably fulfilling the more important role of permanent boundary markers. Ethnographic accounts suggest that many of these boundaries were also planted with fast-growing trees and marked by woven fences (Gifford, 1929:176). This pattern is especially the case in the south-central and eastern districts of Tongatapu, the areas associated with the rise of the Tu'i Tonga dynasty. The more dispersed pattern in the western district of island is somewhat puzzling, given that this is the area said to be the most highly populated at the time of early European contact. This patterning may provide a clue to the relative chronology of mound building on Tongatapu (i.e., an indication that mound construction may have slowed by the 17th–18th Centuries).

Based on accounts from Cook and other early explorers, the basic Tongan residential compound is thought to have included a mound or platform, among other features (Spennemann, 1989:341). Using mounds as a proxy for settlement, we can hypothesize that the pattern of earthworks revealed by our AFE algorithms reflects fundamental elements of traditional Tongan land tenure. Settlement was diffuse within individual territories, but bounded and highly structured at the landscape scale. Chiefs settled their hereditary tracts evenly with commoners, and recognized long-standing, clearly marked territorial boundaries. This kind of segmentation has been described in northern Tonga (Kirch, 1988) but has not been discussed in the context of Tongatapu. Importantly, many of the mound clusters revealed in this study closely correlate with modern Tongan nobles' hereditary estates (*tofi'a*) — an indication that at least some modern political boundaries are derived from ancient land divisions. While major land reforms since the 19th Century have altered the original picture of chiefly holdings, this dataset, at the very least, provides us with the means to estimate the locations of boundaries and residential nodes through time.

5.3. Conclusion

This study presents a first look at an exciting new LiDAR dataset that reveals the remarkably complex archaeological landscape of Tongatapu, the centre of the Classical Tongan Chiefdom (ca. 1000–1850 CE). The intact nature of this landscape owes much to the rural character of the Tongatapu countryside, where traditional mixed-crop agriculture remains the dominant land use. Prospection of monumental and community-scale earthen mounds using LiDAR has helped define the extent and complexity of the sociopolitical landscape of Tonga, which had previously been inferred through extrapolation from small-scale surveys. The DEMs reveal ubiquitous anthropogenic mounds, most of which are known from archaeological and ethnohistorical research to have associations with funerary behaviour and chiefly status.

Two semi-automated feature extraction techniques, object-based image analysis and an inverted pit-filling algorithm (*iMound*) were compared for their efficiency in identifying earthen mounds on Tongatapu. While both techniques successfully detected mounds, *iMound* achieved slightly better results. Both techniques should be considered "coarse" — that is, providing a general spatial pattern rather than accounting for all individual features. Spatial analysis of the mound data generated from AFE show the monumental landscape of Tongatapu to be highly structured.

In-field verification remains an essential component in landscape research. Remote sensing cannot substitute for experience of a site on the ground, nor can it provide the kind of specific contextual information that local informants may hold. Many

mounds in Tonga have names and oral histories associated with them; some are in use to this day for burial. These are critical elements that cannot be "remotely sensed" (Ainsworth et al., 2013). Nevertheless, our use of LiDAR survey has shown that archaeological phenomena can be extracted and analyzed at the landscape scale. The methods demonstrated in this paper provide us with patterns, concentrations, and specific locations to target for more intensive in-field study. The spatial extent of the patterns revealed through this research open the landscape of the Tongan Chiefdom to a level of anthropological inquiry that was not previously attainable.

Funding

This research was supported in part by a Doctoral Fellowship from the Social Sciences and Humanities Research Council of Canada (SSHRC ref. 752-2014-1891), held by Freeland.

Acknowledgments

We are grateful for the close reading and excellent suggestions made by two anonymous reviewers. Errors that remain in this paper are our own. We would like to acknowledge the field support and companionship of Shane Egan and Denis Tu'inukuafe of Tonga, without whom visiting the many mounds and forts of Tongatapu would be very difficult indeed. Kathleen LeBlanc and Kody Huard also provided much appreciated support in the field.

References

AAM Pty Ltd, 2011. Tongatapu and Lifuka Islands Topographic and Bathymetric LiDAR Capture Project. Final Project Report on file with Kingdom of Tonga Ministry of Lands, Survey, and Natural Resources.

Ainsworth, Stewart, Oswald, Al, Went, Dave, 2013. Remote acquired, not remotely sensed: using lidar as a field survey tool. In: Opitz, Rachel S., Cowley, David C. (Eds.), Interpreting Archaeology Topography. Oxbow Books, Oxford, pp. 206–222.

Baatz, Martin, Schäpe, Arno, 2010. Multi-resolution segmentation: an optimization approach for high quality multi-scale image segmentation. In: Strobl, J., et al. (Eds.), Angewandte Geographische Informationsverarbeitung. Wichmann, Heidelberg, Germany, pp. 12–23.

Bennett, Rebecca, Welham, Kate, Hill, Ross A., Ford, Andrew, 2012. A comparison of visualization techniques for models created from airborne laser scanned data. Archaeol. Prospect. 19, 41–48.

Bewley, R.H., Crutchley, S.P., Shell, C.A., 2005. New light on an ancient landscape: lidar survey in the Stonehenge World Heritage Site. Antiquity 79 (305), 636–647.

Bott, Elizabeth, 1982. Tongan Society at the Time of Captain Cook's Visits: Discussions with Her Majesty Queen Salote Tupou. Polynesian Society, Wellington.

Burley, David V., 1996. Sport, status, and field monuments in the Polynesian Chiefdom of Tonga: the pigeon snaring mounds of northern Ha'apai. J. Field Archaeol. 23 (4), 421–435.

Burley, David V., 1998. Tongan archaeology and the Tongan past, 2850–150 BP. J. World Prehist. 12 (3), 337–392.

Challis, Keith, Forlin, Paolo, Kincey, Mark, 2011. A generic toolkit for the visualization of archaeological features on airborne LiDAR elevation data. Archaeol. Prospect. 18, 279–289.

Chase, Arlen F., Chase, Diane Z., Weischampel, John F., Drake, Jason B., Shrestha, Ramesh L., Clint Slatton, K., Awe, Jaime J., Carter, William E., 2011. Airborne LiDAR, archaeology, and the ancient Maya landscape at Caracol, Belize. J. Archaeol. Sci. 38 (2), 387–398.

Chase, Arlen F., Chase, Diane Z., Fisher, Christopher T., Leisz, Stephen J., Weishampel, John F., 2012. Geospatial revolution and remote sensing LiDAR in Mesoamerican archaeology. Proc. Natl. Acad. Sci. 109 (32), 12916–12921.

Chase, Arlen F., Chase, Diane Z., Awe, Jaime J., Weischampel, John F., Iannone, Gyles, Moyes, Holly, Jaeger, Jason, Brown, Kathryn, Shrestha, Ramesh L., Carter, William E., Fernandez-Diaz, Juan, 2014. Ancient Maya regional settlement and inter-site analysis: the 2013 West-Central Belize LiDAR Survey. Remote Sens. 6, 8671–8695. http://dx.doi.org/10.3390/rs6098671.

Clark, Geoffrey, 2014. Social memory and the langi (royal tombs) of Lapaha, Tonga. In: Martinsson-Wallin, Helene, Thomas, Timothy (Eds.), Monuments and People in the Pacific. Department of Archaeology and Ancient History, Uppsala University, pp. 221–244. Studies in Global Archaeology no. 20.

Clark, Geoffrey, 2015. Chiefly tombs, lineage history and the ancient Tongan state. J. Isl. Coast. Archaeol. http://dx.doi.org/10.1080/15564894.2015.1098754.

Clark, Geoffrey, Reepmeyer, Christian, 2014. Stone architecture, monumentality, and the rise of the early Tongan chiefdom. Antiquity 88, 1244–1260.

Clark, Geoffrey, Burley, David V., Murray, Tim, 2008. Monumentality and the development of the Tongan maritime chiefdom. Antiquity 82, 994–1008.

Cowley, David C., 2012. In with the new, out with the old? Auto-extraction for remote sensing in archaeology. In: Bostater Jr., Charles R., Mertikas, Stelios P., Neyt, Xavier, Nichol, Caroline (Eds.), SPIE Proceedings Vol. 8532 Remote Sensing of the Ocean, Sea Ice, Coastal Waters, and Large Water Regions 2012. Dave Cowley, and Jean-Paul Bruyant, Edinburgh, UK.

Davidson, Janet M., 1969. Archaeological excavations in two burial mounds at 'Atele, Tongatapu. Rec. Auckl. Inst. Mus. 6, 251–286.

De Laet, V., Paulissen, E., Waelkens, M., 2007. Methods for the extraction of archaeological features from very high-resolution Ikonos-2 remote sensing imagery, Hisar (southwest Turkey). J. Archaeol. Sci. 34 (5), 830–841.

Evans, Damian H., Fletcher, Roland J., Pottier, Christophe, Chevance, Jean-Baptiste, Soutif, Dominique, Suy Tan, Boun, Im, Sokrithy, Ea, Derith, Tin, Tina, Kim, Samnang, Cromarty, Christopher, Greef, Stéphane de, Hanus, Kasper, Bâty, Pierre, Kuszinger, Robert, Shimoda, Ichita, Boornazian, Glenn, 2014. Uncovering archaeological landscapes at Angkor using lidar. Proc. Natl. Acad. Sci. 110 (31), 12595–12600.

Fernandez-Diaz, Juan, Carter, William E., Shrestha, Ramesh L., Glennie, Craig L., 2014. Now you see it… now you don't: understanding airborne mapping LiDAR collection and data product generation for archaeological research in Mesoamerica. Remote Sens. 6, 9951–10001.

Fernández-Lozanoa, Javier, Gutiérrez-Alonsoa, Gabriel, Fernández-Moránd, Miguel Ángel, 2015. Using airborne LiDAR sensing technology and aerial orthoimages to unravel Roman water supply systems and gold works in NW Spain (Eria valley, León). J. Archaeol. Sci. 53, 356–373.

Gifford, Edward Winslow, 1929. Tongan Society. Bernice P. Bishop Museum, Honolulu. Bulletin no. 61.

Glennie, Craig L., Carter, Wialliam E., Shretha, Ramesh L., Dietrich, William E., 2013. Geodetic imaging with airborne LiDAR: the earth's surface revealed. Rep. Prog. Phys. 76 (8) http://dx.doi.org/10.1088/0034-4885/76/8/086801.

Hanus, Kasper, Evans, Damian, 2015. Imaging the waters of Angkor: a method for semi-automated pond extraction from LiDAR data. Archaeol. Prospect. http://dx.doi.org/10.1002/arp.1530.

Herda, Phyllis S., 1988. The Transformation of the Traditional Tongan Polity: a Genealogical Consideration of Tonga's Past. Unpublished PhD dissertation. Australian National University, Canberra.

Hesse, Ralf, 2010. LiDAR-derived local relief models: a new tool for archaeological prospection. Archaeol. Prospect. 17, 67–72.

Kirch, Patrick V., 1988. Niuatoputapu: the Prehistory of a Polynesian Chiefdom. Burke Museum, Seattle.

Kirch, Patrick V., 1990. Monumental architecture and power in polynesian chiefdoms: a comparison of Tonga and Hawaii. World Archaeol. 22 (2), 206–222.

Kvamme, Kenneth, 2013. An examination of automated archaeological feature recognition in remotely sensed imagery. In: Bevan, Andrew, Lake, Mark (Eds.), Computational Approaches to Archaeological Spaces. Left Coast Press, Walnut Creek, CA, pp. 53–68.

Ladefoged, Thegn N., McCoy, Mark D., Asner, Gregory P., Kirch, Patrick V., Puleston, Cedric O., Chadwick, Oliver A., Vitousek, Peter M., 2011. Agricultural potential and actualized development in Hawaii: an airborne lidar survey of the leeward Kohala field system (Hawaii Island). J. Archaeol. Sci. 38, 3605–3619.

Li, S., MacMillan, R.A., Lobb, D.A., McConkey, B.G., Moulin, A., Fraser, W.R., 2011. Lidar DEM error analyses and topographic depression identification in a hummocky landscape in the prairie region of Canada. Geomorphology 129, 263–275.

Luo, Lei, Wang, Xinyuan, Guo, Huadong, Liu, Chuansheng, Liu, Jie, Li, Li, Du, Xiaocui, Qian, Guoquan, 2014. Automated extraction of the archaeological tops of qanat shafts from VHR imagery in Google earth. Remote Sens. 6, 11956–11976.

McCoy, Mark D., Asner, Gregory P., Graves, Michael W., 2011. Airborne lidar survey of irrigated agricultural landscapes: an application of the slope contrast method. J. Archaeol. Sci. 38, 2141–2154.

McKern, William C., 1929. Archaeology of Tonga. Bernice P. Bishop Museum, Honolulu, Hawaii. Bulletin no. 60.

Planchon, O., Darboux, F., 2001. A fast, simple, and versatile algorithm to fill the depressions of digital elevation models. Catena 46, 59–176.

Prufer, Keith M., Thompson, Amy E., Kennett, Douglas J., 2015. Evaluating airborne LiDAR for detecting settlements and modified landscapes in disturbed tropical environments at Uxbenká, Belize. J. Archaeol. Sci. 57, 1–13.

Quintus, Seth, Clark, Jeffrey T., Day, Stephanie S., Schwert, Donald P., 2015. Investigating regional patterning in archaeological remains by pairing extensive survey with a lidar dataset: the case of the Manu'a Group, American Samoa. J. Archaeol. Sci. Rep. 2, 677–687.

R Development Core Team, 2012. R: a Language and Environment for Statistical Computing. R Foundation for Statistical Computing, Vienna, Austria. Available at: http://www.R-project.org (verified 28 October 2014).

Riley, Melanie A., 2009. Automated Detection of Prehistoric Conical Burial Mounds from LiDAR Bare-earth Digital Elevation Models. Unpublished MA thesis. Department of Geology and Geography, Northwest Missouri State University, Maryville.

Rochelo, Mark J., Davenport, Christian, Selch, Donna, 2015. Revealing pre-historic native American Belle Glade earthworks in the northern Everglades utilizing airborne LiDAR. J. Archaeol. Sci. Rep. 2015 (2), 624–643.

Schneider, Anna, Takla, Melanie, Nicolay, Alexander, Raab, Alexandra, Raab, Thomas,

2014. A template-matching approach combining morphometric variables for automated mapping of charcoal kiln sites. Archaeol. Prospect. http://dx.doi.org/10.1002/arp.1497.
Spennemann, Dirk H.R., 1989. 'Ata 'a Tonga mo 'ata 'o Tonga: Early and Later Prehistory of the Tongan Islands. PhD dissertation. Department of Prehistory, Australian National University, Canberra.
Stantis, C., Kinaston, R.L., Richards, M.P., Davidson, J.M., Buckley, H.R., 2015. Assessing human diet and movement in the Tongan maritime chiefdom using isotopic analyses. PLoS One 10 (3), e0123156. http://dx.doi.org/10.1371/journal.pone.0123156.
Štular, Benjamin, Kokalj, Žiga, Oštir, Krištof, Nuninger, Laure, 2012. Visualization of lidar-derived relief models for detection of archaeological features. J. Archaeol. Sci. 39, 3354–3360.
Swanson, Lynn, 1968. Field Monuments of Tongatabu. Unpublished Manuscript on File. Department of Anthropology, University of Auckland, Auckland.
Trier, Øivind Due, Pilø, Lars Holger, 2012. Automatic detection of pit structures in airborne laser scanning data. Archaeol. Prospect. 19, 103–121.
Trier, Øivind Due, Larsen, Siri Øyen, Solberg, Rune, 2009. Automatic detection of circular structures in high resolution satellite images of agricultural land. Archaeol. Prospect. 16, 1–15.
Urbanowicz, Charles F., 1977. Motives and methods: missionaries in Tonga in the early 19th century. J. Polyn. Soc. 86 (2), 245–263.
Van Rijsbergen, C.J., 1979. Information Retrieval. Butterworths, London.
Wang, L., Liu, H., 2006. An efficient method for identifying and filling surface depressions in digital elevation models for hydrologic analysis and modelling. Int. J. Geogr. Inf. Sci. 20, 193–213.